Viral rebound kinetics following single and combination immunotherapy for HIV/SIV

M. Prague[1], J.M. Gerold[2], I. Balleli[1], C. Pasin[1], J.Z. Li[3], D.H. Barouch[4], J.B. Whitney[4], A.L. Hill[2]

[1]Inria, Inserm U1219 BPH, SISTM team, University of Bordeaux, France. [2]Program for Evolutionary Dynamics, Harvard University, Cambridge, USA. [3]Brigham and Women's Hospital, Boston, MA, USA. [4]Beth Israel Deaconess Medical Center, Boston, MA, USA.

Abstract

Immunotherapy is a promising approach to prevent or control HIV rebound following cessation of antiretroviral therapy (ART). We conducted an in-depth characterization of viral load kinetics following ART interruption across multiple studies of TLR7-agonist treatment, in combination with therapeutic vaccination or broadly neutralizing antibodies, in SIV- or SHIV-infected macaques. To quantify rebound kinetics and the effects of immunotherapy, we developed a viral dynamics model that includes stochastic reactivation from latency and adaptive immune responses.

Study Design & Data

Three recent studies administered TLR7-based immunotherapy to rhesus macaques suppressed on ART, followed by treatment interruption. In total these studies included 100 animals receiving 10 different treatment combinations. We performed a unified, model-driven analysis of these data kinetics in order to assess how each treatment impacted viral rebound. (**Fig. 1**).

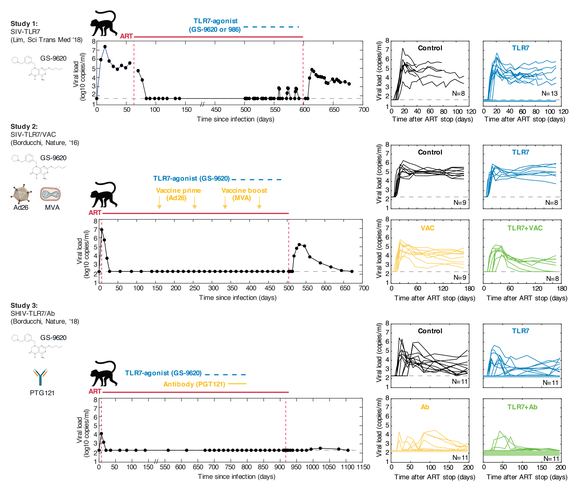

Fig. 1: Study Designs Overview.

- Study 1: Control, TLR7 Agonist GS-9620 or GS-986. ART at 9 weeks. 8 control and 13 treated macaques
- Study 2: Control, TLR7 Agonist GS-9620, Vaccine Ad26/MVA, or Combination. ART at 1 week. 9 macaques in each group (34 total)
- Study 3: Control, TLR7 Agonist GS-9620, Antibody PGT121, or Combination. ART at 1 week. 11 macaques in each group (44 total)

Funding

This work was supported by NIH grants DP5OD019851 (ALH), P01AI131365 (ALH, JBW), and P01AI131385 (ALH, MP), and P30AI060354 (Harvard CFAR; ALH, JG), as well as funding from the French National Institute for Research in Computer Science and Automation (Inria) through an International Associate Team award (MP, ALH). Contact: alhill@fas.harvard.edu

Viral Dynamics Model

Mechanistic mathematical models are a well-established tool for characterizing and quantifying the dynamics of HIV/SIV infection within individual hosts. However, standard models of viral rebound fail to capture the range of dynamic behaviors observed in these studies. We developed an expanded model of viral dynamics to include an adaptive immune response and latency reactivation (**Fig. 2, 3**).

Instead of directly estimating a, the effective rate at which cells reactivate from the latent reservoir, we estimated t_a, the average waiting time between reactivation events and used a formula to transform it into a to go into the model equations. The transformation was designed so that it worked in both the regime of frequent, deterministic reactivation associated with larger reservoir sizes and rare, stochastic reactivation from smaller reservoir sizes

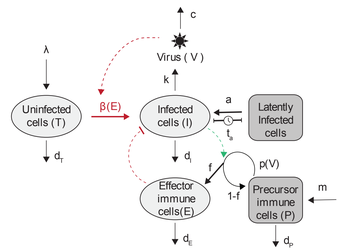

Fig. 2: Expanded model of viral dynamics. Virus v infects target cells T which become infected cells I and in turn produce virus. Immune precursor cells P interact with I and proliferate, giving rise to effector cells E, which inhibit infection. Finally, latently infected cells can restart infection by exiting from latency with rate a (or equivalently, every t_a days on average).

$$\dot{\mathbf{T}} = \lambda - \beta \mathbf{T}\mathbf{V} - d_T\mathbf{T}$$
$$\dot{\mathbf{I}} = a + \frac{\beta \mathbf{T}\mathbf{V}}{1 + (\mathbf{E}/N_E)} - d_I\mathbf{I}$$
$$\dot{\mathbf{V}} = k\mathbf{I} - c\mathbf{V}$$
$$\dot{\mathbf{P}} = m + p(1-f)\mathbf{P}\frac{\mathbf{V}}{\mathbf{V}+N_p} - d_P\mathbf{P}$$
$$\dot{\mathbf{E}} = pf\mathbf{P}\frac{\mathbf{V}}{\mathbf{V}+N_p} - d_E\mathbf{E}$$

Fig. 3: System of differential equations describing infection dynamics.

- $\mathbf{T}$, target cells.
- $\mathbf{I}$, infected cells.
- $\mathbf{V}$, free virus.
- $\mathbf{P}$, immune precursors.
- $\mathbf{E}$, immune effectors.

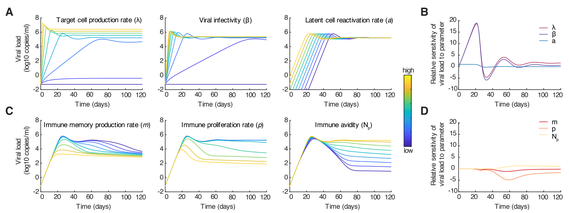

Fig. 4: Impact of kinetic parameters on viral rebound A,C) Viral load trajectories produced by the model when varying a single parameter. Top row: weak immune response. Bottom row: stronge immune response. The availability of target cells (λ) and the baseline viral infectivity (β) control the early viral growth rate, while the timing of rebound depends on the rate at which latent cells reactivate (a). A strong adaptive immune response can curtail rebound. The size and timing of peak viremia is determined by the expansion rate of immune effectors (p) and the memory pool at ART stop (m). The degree of control of the setpoint viral load is determined mainly by N_P, the viral load level at which antigen-stimulation is half-maximal. B,D) Relative ensitivity of viral load to parameter values over time ($\frac{\partial V}{\partial \theta}\frac{\theta}{V}$).

Results

To fit the model to viral rebound kinetics in each animal and evaluate potential treatment differences between groups in a statistically rigorous way, we used a mixed-effects modeling framework implemented in Monolix. We fit parameters $\beta, \lambda, a, m, p, N_p$, allowing each to have group-level effects and random (individual-level) effects. Other parameters were fixed at values from the literature. We tested for treatment effects of immunotherapy (TLR7, Vac, Ab) and timing of ART initiation (early vs late) on each parameter, using a combined forward-backward selection approach, to choose the model with best Bayesian Information Criterion. SIV- and SHIV-infected animals were fit separately.

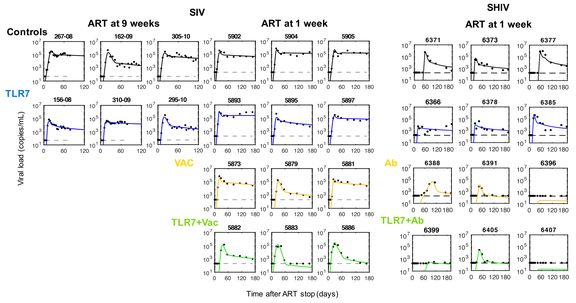

Fig. 5: Example model fits. The model can describe the wide range of rebound kinetics observed in the studies, including delayed rebound and post-treatment control.

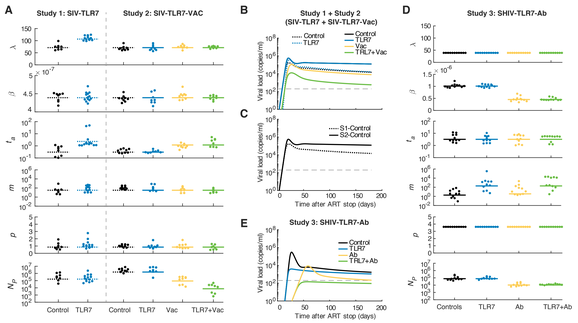

Fig. 6: Treatment effects estimated from model fitting. A,D): Individual and group mean parameter estimates. B-E): Simulated viral load trajectories with group mean parameters.

Summary of infered treatment effects

- Late ART initiation: 10-fold increase in immune response avidity (↓ N_P)
- TLR7-agonist
  - 8-fold reduction in LR activation (↑ t_a) (late ART only)
  - 1.5-fold increase in target cell density (↑ λ) (late ART only)
  - 175-fold increase in immune avidity (↓ N_P) (when w/vaccine)
  - 100-fold increase in memory pool (↑ m) (in SHIV only)
- Vaccine
  - 4-fold reduction in LR reactivation (↑ t_a)
  - 18-fold boost in immune avidity (↓ N_P)
- Antibody
  - 7-fold boost in immune avidity (↓ N_P)
  - 2-fold reduction in viral infectivity (↓ β)

Predicting Effects in Humans

Non-human primate studies are conducted with the hope that outcomes in this animal model are a good predictor of outcomes in human clinical trials. We developed a method to predict how viral rebound kinetics under immunotherapy will translate from macaques to HIV-infected humans, taking into account baseline differences in rebound. First we calibrated our model to HIV rebound, using data from 70 patiens undergoing ART interruption (ACTG5024, 5068, 5197) (**Fig. 7**). Then we simulated the effect of adding TLR7-agonist, vaccine, or Ab based on effects identified in the SIV and SHIV studies (**Fig. 8**). The highly context-dependent impact of TLR7 on rebound kinetics in macaques suggests these results should be interpreted with caution.

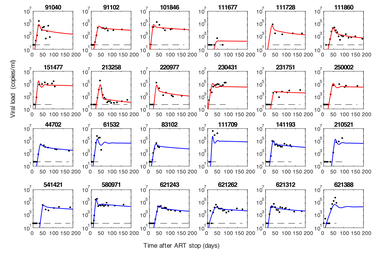

Fig 7: Example models fits to HIV rebound. Individuals in red were treated with non-NNRTI based antiretroviral therapy, while individuals in blue were treated with NNRTI-based regimes (infered to lead to 3 day delay in drug washout time at group level).

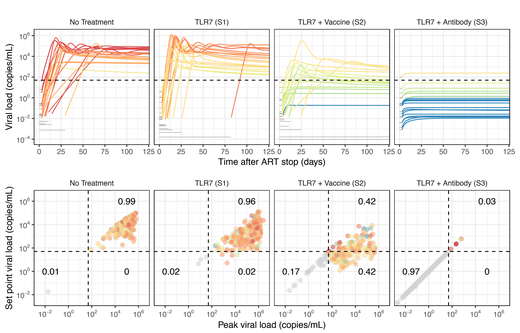

Fig 8: Simulated HIV rebound after immunotherapeutic treatment in humans. Top row: 20 example rebound trajectories colored by viral load. Bottom row: 200 simulated individuals plotted by their peak and final rebound viral loads, colored by time of rebound.

Conclusions

We developed a mathematical modeling framework for viral rebound which can capture a wide range of kinetics observed in SIV, SHIV, and HIV infection. This model includes stimulation of an adaptive immune response and stochastic delays to reactivation of latently infected cells. Our analysis suggested that the success of TLR7-based immunotherapies was mainly due to their ability to boost antiviral immune responses, with a smaller role played by reduction in the latent reservoir. We found that TLR7-agonists had a multi-faceted impact on rebound which was highly dependent on the context (specific virus, timing of ART initiation, and combination with other therapies), limiting the ability to translate results to HIV.